Impact of climate change on the streamflow of the Arjo-Didessa catchment under RCP scenarios

Wudeneh Temesgen Bekele, Alemseged Tamiru Haile and Tom Rientjes

ABSTRACT

In this study, the impact of climate change on the streamflow of the Arjo-Didessa catchment, Upper Blue Nile basin, is evaluated. We used the outputs of four climate models for two representative concentration pathway (RCP) climate scenarios, which are RCP 4.5 and RCP 8.5. Streamflow simulation was done by using the HEC-HMS rainfall-runoff model, which was satisfactorily calibrated and validated for the study area. For the historic period (1971–2000), all climate models significantly underestimated the observed rainfall amount for the rainy season. We therefore bias-corrected the climate data before using them as input for the rainfall-runoff model. The results of the four climate models for the period 2041 to 2070 show that annual rainfall is likely to decrease by 0.36 to 21% under RCP 4.5. The projected increases in minimum and maximum temperature will lead to an increase in annual evapotranspiration by 3 to 7%, which will likely contribute to decreasing the annual flows of Arjo-Didessa by 1 to 3%. Our results show that the impact is season dependent, with an increased streamflow in the main rainy season but a decreased flow in the short rainy season and the dry seasons. The magnitudes of projected changes are more pronounced under RCP 8.5 than under RCP 4.5.

Key words | Arjo-Didessa, climate change, HEC-HMS, RCM, streamflow, Upper Blue Nile

Wudeneh Temesgen Bekele (corresponding author)
Arba Minch Water Technology Institute,
Arba Minch University,
P. O. Box 21, Arba Minch,
Ethiopia
E-mail: *temsgwudeneh@gmail.com*

Alemseged Tamiru Haile
International Water Management Institute (IWMI),
P. O. Box 5689, Addis Ababa,
Ethiopia

Tom Rientjes
Department of Water Resources,
ITC,
P.O. Box 6, 7500AA Enschede,
The Netherlands

HIGHLIGHTS

- Hydrological modeling was done by using HEC-HMS.
- Outputs of four regional climate models were bias-corrected for hydrological impact evaluation.
- For the period 2041 to 2070, annual rainfall will decrease by 0.36 to 21%, while the annual PET will increase by 3 to 7% under RCP 4.5.
- The annual flows of Arjo-Didessa will decrease by 1 to 3%.
- The impact is season dependent, with an increased streamflow in the main rainy season.

doi: 10.2166/wcc.2021.307

GRAPHICAL ABSTRACT

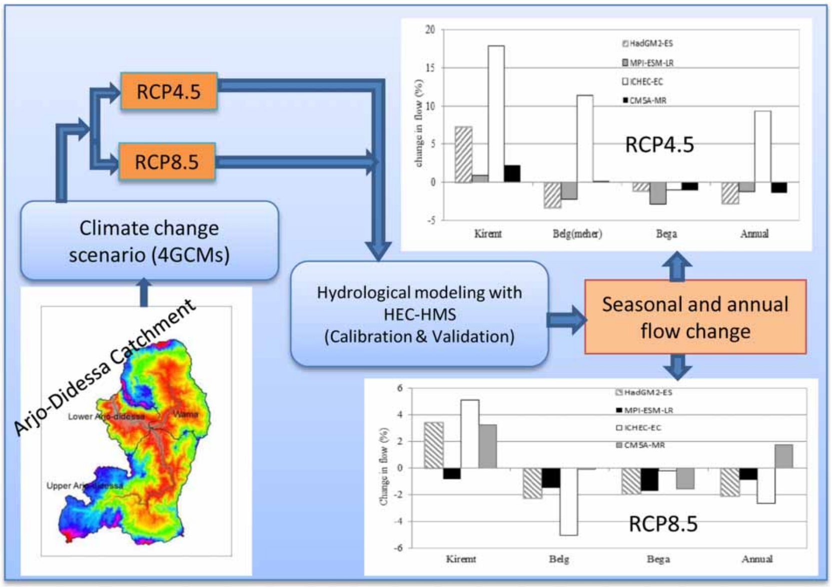

INTRODUCTION

The fifth Assessment Report (AR5) of the Intergovernmental Panel on Climate Change (IPCC) indicates that rainfall over Eastern Africa has decreased between March and June in the last three decades, while there has been an increase in temperature over East Africa since the beginning of the 1980s. Climate projections also indicate that there will be a likely increase in rainfall amount and extreme rainfall in the region by the end of the 21st century. There will be higher rates of evaporation in Ethiopia due to warming over the country. Such changes are expected to impact the economy of East African countries, including Ethiopia, by high climate sensitivity (Change 2014).

Many studies reported the impact of climate change on the streamflow of the meso-scale Upper Blue Nile (UBN) basin (176,000 km^2) under the Special Report Emission Scenario (SRES). Beyene *et al.* (2010) and Elshamy *et al.* (2009) reported that the flow of UBN is likely to decline by the end of the century. Setegn *et al.* (2011) concluded that a significant decline in the annual streamflow of the Lake Tana sub-basin is expected. The magnitude of floods in the UBN is expected to be more severe (Kim & Kaluarachchi 2009; Nawaz *et al.* 2010), while the direction of projected changes of the dry season flows of the UBN basin is not clear (Taye *et al.* 2015; Enyew *et al.* 2014).

Hydrological impact assessment on UBN streamflow based on representative concentration pathway (RCP) scenarios has been studied only by a few. Aich *et al.* (2014) studied the implication of RCP 2.6 and RCP 8.5 by focusing on extreme flows. Haile *et al.* (2017) evaluated the future changes in the average flow of 19 catchments in UBN under the RCP 4.5 scenario. Chakilu *et al.* (2020) evaluated the extent to which climate change is happening and its impacts on the streamflow of the Gumara watershed under the RCP climate change scenarios. The study considered the RCP 2.6, RCP 4.5, and RCP 8.5 scenarios using the second-generation Canadian Earth System Model (CanESM2) and concluded that, due to climate change, the streamflow of the watershed is found to be increasing by 4.06, 3.26, and 3.67% under the RCP 2.6, RCP 4.5, and RCP 8.5 scenarios, respectively. Mengistu *et al.* (2020) used the CCLM regional climate model (RCM) to assess the climate change impacts on the UBN River basin by projections of increases in mean annual temperature and decrease in precipitation in most parts of the basin. They concluded that the total water yield of the basin is estimated to decrease by 1.7 to 6.5% and 10.7 to 22.7%, for simulations forced by the RCP 4.5 and RCP 8.5 scenarios, respectively. This indicates that climate change has different impacts on a small scale than on a large scale.

Taye *et al.* (2015) reviewed recent studies on the implication of climate change on hydrological extremes in the Blue Nile basin. They concluded that most studies show that the consistent increase in temperature might lead to an increase in potential evapotranspiration (PET) and a reduction in annual streamflow in the 21st century.

Studies indicated that future changes (2071–2100) in climate will affect existing and planned water resources projects in the sub-basins of UBN (McCartney & Menker Girma 2012). Projected changes in rainfall and streamflow are also different when evaluated in the entire UBN and its sub-basins (Taye *et al.* 2015; Haile *et al.* 2017). For example, as we included above, the investigation done by Chakilu *et al.* (2020) over the Gumara watershed (found in the UBN) concluded that there will be an increasing streamflow change, while Mengistu *et al.* (2020) concluded that there will be a decreasing mean streamflow up to 22.7% over the UBN River basin. Roth *et al.* (2018) agreed with Chakilu *et al.* (2020) that streamflow from the Blue Nile basin could increase by 21 to 97%. Taye *et al.* (2015), using general circulation model (GCM) outputs under the SRES scenario, showed a reduction of streamflow of the UBN, and Kim & Kaluarachchi (2009), using six GCMs and two tank hydrological models, concluded that low flows may become higher. Similarly, Shaka (2008) evaluated the climate change impact on the Gilgel Abay catchment using the HBV model and the single GCM climate model and concluded that runoff will decrease by 12% in the main rainy season.

Although some studies were done on the UBN and its sub-basin using the RCM, different projected streamflow magnitudes were observed between them. This is mainly due to most studies using a single climate model. For example, Teklesadik *et al.* (2017), using the RCP scenario and the RCM, showed that the mean annual discharge increased by 6.6% for the period 2070 to 2099; Gebre *et al.* (2015) showed that the average annual runoff volume may increase up to 127.4% in the 2070s. Also, Gelete *et al.* (2020) reviewed many studies over the Blue Nile River basin and reviled that the average annual temperature and evapotranspiration will increase by 19.1 and 12.6%, respectively, while rainfall is expected to decrease by 15.3% in 2100 and the flow is also likely to decrease. Similarly, Tariku *et al.* (2021) showed the impact of climate change on hydrology and hydrologic extremes of the Upper Blue Nile River basin using three hydrological models and four climate models under the RCP 4.5 and RCP 8.5 scenarios. The author concludes that the potential global warming impact on the extreme and mean streamflows of the UBN River basin was projected to decrease by 7.6% in 2050s and in the 2080s.

As stated above, most scientific investigations focused on the use of outputs from single climate models. These studies mostly addressed the impact of climate change on a large scale such as the Blue Nile basin. However, there is a lack of evidence on the local impacts of climate change despite the recent availability of high-resolution climate projections from RCMs. Previous studies on the Arjo-Didessa catchment also rely on change projections of a single GCM data based on the SRES emission scenarios (Kim & Kaluarachchi 2009; McCartney & Menker Girma 2012; Gebre *et al.* 2015). GCMs provide projections at coarse spatial resolution in the order of 300 km × 300 km, and it is a major constraint to local-scale hydrological impact assessments (see Tisseuil *et al.* 2010; Teutschbein & Seibert 2012). Sub-grid scale features such as topography, clouds and land use, and their effects on predictor values are not well represented. As a result, there is a need to use RCM outputs with a spatial grid resolution of 50 km × 50 km. We therefore evaluated the implications of the RCP scenarios on water availability in the Arjo-Didessa catchment of the UBN by considering multiple RCMs. We intercompare the projections of single models to maintain consistency in the projections, address the inconsistency in the projections and resolve the ambiguity of impact assessments. The results are compared against previously reported results for the region.

MATERIALS AND METHODS

Study area

The Arjo-Didessa catchment is the upper part of the Didessa sub-basin which is situated in the southern part of the UBN basin, Ethiopia. The catchment covers a geographical area of 7°53′ and 9°0′N latitude and 35°50′ and 37°0′E longitude (Figure 1). Arjo-Didessa has an estimated drainage area of about 9,997 km^2 with two main sub-catchments, namely, the Wama and Upper Arjo-Didessa sub-catchments. The average annual flow of Arjo-Didessa is 76.64 $m^3 s^{-1}$, which is equivalent to 15.81 Mm^3 of water volume.

According to the Ethiopian climate classification based on elevation (i.e. <500 m: Bereha; 500–1,500: Kola; 1,500–2,440: Weina Dega; and >2,440: Dega), most parts of the Arjo-Didessa catchment fall under the Weina Dega (moderate climatic condition) climate zone with a mean annual rainfall of 1,971 mm for the period 1981–2013. It has a small mountain which is characterized by the Dega climate zone (cool climatic condition) with an annual average rainfall of about 1,672 mm. The valley along the two main rivers is within the Kola zone (tropical) with an annual average rainfall of about 1,900 mm. The overall mean annual catchment rainfall is about 1,779 mm. The mean maximum and minimum temperature of the Arjo-Didessa catchment is 24.29 and 12.15 °C, respectively, with a mean annual temperature of 18 °C. The average annual evapotranspiration of the catchment is 1,453 mm.

Dataset

Historical climate data such as rainfall, wind speed at 2 m height, sunshine hour, maximum and minimum temperature, and relative humidity of the study area were collected from the National Meteorology Agency (NMA) of Ethiopia. These data have daily temporal resolution and cover the time period 1981–2008. Dynamically downscaled climate

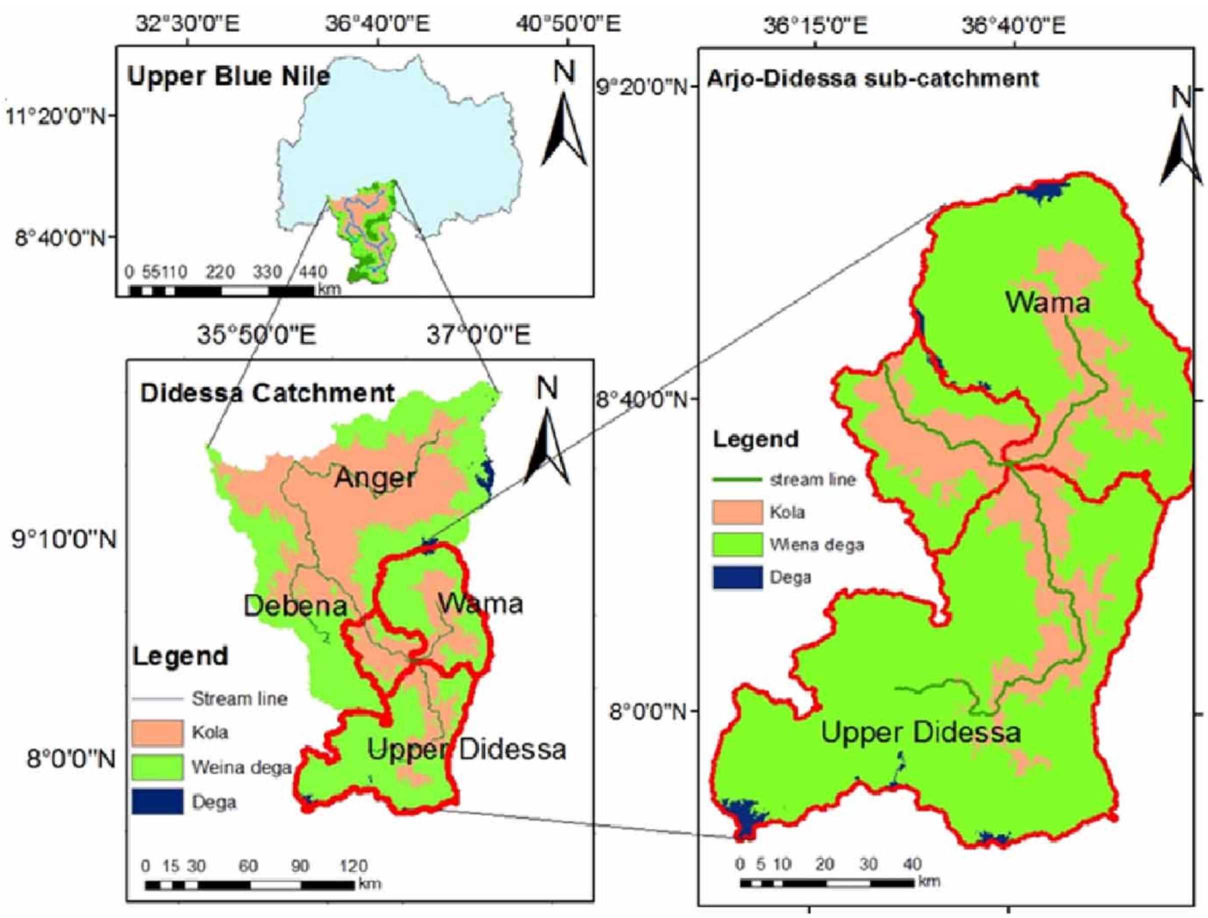

Figure 1 | Geographic features of the study area and its climate zones.

data were obtained by using the CORDEX-Africa program (http://wcrp-cordex.ipsl.jussieufr) for two RCP scenarios: RCP 4.5 and RCP 8.5. RCP 8.5 is a high emission scenario, while RCP 4.5 is an intermediate reference scenario (Thomson *et al.* 2011; Rogelj *et al.* 2012). Scenarios indicate radiative forcing values in W/m^2.

The CORDEX-Africa program provided climate data that were simulated by four GCMs (HadGM2-ES, MPI-ESM-LR, ICHEC-EC, and CM5A-MR) and dynamically downscaled by three RCMs, which are Regional Climate Limited-area modeling (CCLM), Rossby Center regional atmospheric model (RCA4), and KNMI Regional Atmospheric Climate Model, version 22 (RAMO22 T). More information is presented in Table 1.

Daily streamflow data (from 1981 to 2008), land use/cover, and soil data of the Arjo-Didessa catchment were collected from the Ministry of Water, Irrigation and Electricity (MoWIE) of Ethiopia. The land cover map was generated in 2001. The daily time series of rainfall and streamflow were screened and corrected for completeness and unexpected values. There was an unrealistic recorded value of flow as high as $1,054\ m^3\ s^{-1}$ that was ignored for further use (Figure 2). Thereafter, to minimize bias during the estimation of missing values, we used the flow time series with the missing value. Then, the missing part was ignored when estimating performance measuring values. The consistency of the daily rainfall time series was evaluated by using a double mass curve analysis. There was no inconsistency of station rainfall time series.

Evaluation of simulated rainfall by climate models

For the time period (1981 to 2000), the downscaled climate rainfall data from the selected climate models were

Table 1 | General description of GCMs, RCMs, and their climate centers

GCMs			RCMs		
Model	**Full name**	**Resolution (km)**	**Model**	**Full name**	**Climate center**
HadGM2-ES	Hadley Global Environment Model 2-Earth System	145 × 192	CCLM	Regional Climate Limited-area Modeling	Met Office Hadley Center
MPI-ESM-LR	Max Planck Institute, Earth System Modeling, Low Resolution	96 × 192	CCLM	Regional Climate Limited-area Modeling	Max Planck Institute for Meteorology (MPI-M)
ICHEC-EC	Irish Center for High-End Computing Earth Consortium	16 × 125	RAMO22T	KNMI Regional Atmospheric Climate Model, version 22	EC-EARTH Consortium
CM5A-MR	Coupled Model Version 5, Medium Resolution	143 × 144	RCA4	Rossby Center regional Atmospheric model	Institute Pierre-Simon Laplace

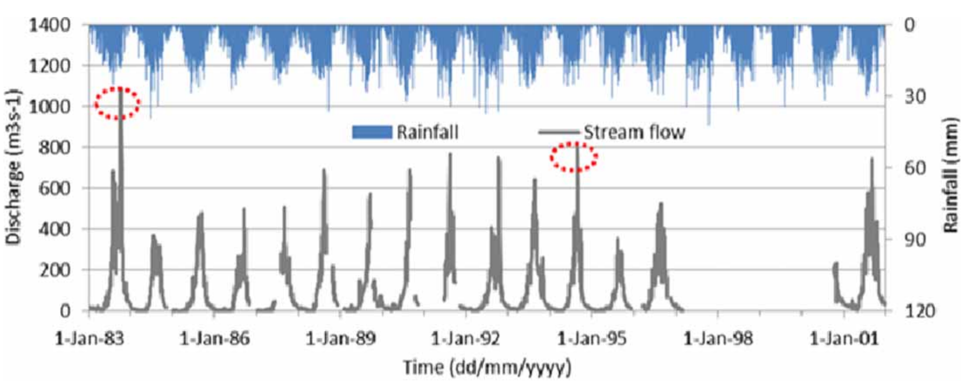

Figure 2 | Graph of streamflow and rainfall data so as to screen streamflow data.

evaluated using statistical measures. These include root mean square error (RMSE), correlation coefficient (CC), coefficient of variation (CV), and bias.

The root-mean-square deviation (RMSD), or RMSE, is a frequently used measure of the differences between values (sample or population values) predicted by a model or an estimator and the values observed. The RMSE represents the square root of the second sample moment of the differences between predicted values and observed values or the quadratic mean of these differences, while CC measures the strength of the linear relationship between observed and simulated rainfall amounts. CV is a measure of the variability of observed or simulated rainfall amounts. Bias indicates the systematic error of the simulated rainfall.

Bias correction

In this study, simulated precipitation and temperature data were bias-corrected before being used as an input to runoff modeling. The temperature was bias-corrected by the linear shifting and scaling method (Terink *et al.* 2010).

$$T_{corr} = \bar{T}_{obs} + \frac{\sigma(T_{obs})}{\sigma(T_{rcm})}(T_{rcm} - \bar{T}_{obs}) + (\bar{T}_{obs} - \bar{T}_{rcm}) \tag{1}$$

where T_{corr} is the corrected daily temperature (°C); T_{rcm} is the simulated daily temperature from the RCM; and T_{obs} is the observed daily temperature, while $\bar{T}_{obs}$ is the mean observed temperature and $\bar{T}_{rcm}$ is the mean simulated temperature.

The simulated precipitation data were also bias-corrected by using a nonlinear correction method. This method results in the mean and standard deviation of the daily precipitation distribution becoming equal to those of the observed distribution (e.g. Lafon *et al.* 2013). The equation reads:

$$P^* = aP^b \tag{2}$$

where P^* is the corrected value of the variable (precipitation), b is the scaling exponent, and a is the coefficient that is determined from the mean of observed rainfall data and the mean of P^b.

HEC-HMS model calibration and validation

In this study, 2 years of daily data (1981 to 1982) were used for warming the HEC-HMS (version 4.1) model. Model calibration at a daily time step covered 19 years (1983 to 2001). This long period facilitated model calibration for different hydrologic regimes (wet, dry, and normal periods). To guide the calibration procedure, sensitive parameters were identified first by running the model for different values of a certain parameter, while keeping the other parameters constant. This was followed by manual calibration, which involved a manual adjustment of the most sensitive parameters' values until a satisfactory match was achieved between observed and simulated streamflow.

The model was then tested (validated) for its performance outside the calibration period. The validation period covered 7 years (2002 to 2008). This period contained wet, dry, and normal periods of the study area.

Deficit and constant loss method, soil conservation service (SCS) unit hydrograph, constant monthly base flow, and Muskingum routing methods of HEC-HMS were used for model simulation. The deficit and constant loss method was used for continuous soil moisture simulation. This method uses a single soil layer to account for continuous changes in moisture content (Saleh *et al.* 2011). The deficit and constant loss method is similar to the initial and constant loss method, except for the fact that the initial loss can be recovered after a prolonged period of no rainfall (Razmkhah *et al.* 2014). This method has four parameters, namely, initial moisture deficit, maximum moisture deficit, constant loss rate, and impervious percentage. The percentage impervious was specified as 0% for our study area, since there were no significant urban settlements. The remaining three parameters were estimated by model calibration.

The SCS unit hydrograph transform method was used to compute direct runoff from excess precipitation. The SCS unit hydrograph is a parametric unit hydrograph model, based on the averages of unit hydrograph derived from gauged rainfall and runoff. The main parameter of this method is basin lag, which is estimated as 0.6 times the time of concentration of the flow. The time of concentration was estimated based on the sub-basin characteristics including terrain slope and the length of the reach (Kirpich's formula).

The constant monthly base flow method was used to account for base flows. This method allows the specification of a constant base flow for each month of the year.

The Muskingum routing method was used to route the flow in reaches using a simple conservation of mass approach. This routing method approximates storage in a system according to a wedge method (Rui & Wang 2000). The development of the wedge is due to a flood wave that causes inflow to exceed outflow and creates a wedge of storage (Chow et al. 1988). It considers a linear relationship between inflow and outflow. The Muskingum method requires three parameters: K, X, and the number of subreaches. K represents the travel time through the reach, while X is the weighting between inflow and outflow influence; it ranges from 0 to 0.5.

In this study, the value of K was initially fixed based on the length of reach and the mean velocity ($V = 1.84$ m/s) which was computed using HEC-GeoHMS software. The final value of K was then determined through calibration. Muskingum X parameter was set at the default value of 0.2, since it was found that the model outputs were not sensitive to this parameter.

Model performance evaluation

The most straightforward possibility of evaluating model performance is a visual inspection of the observed and simulated hydrograph. This graphical technique provides an initial general overview. In this case, the inspection of the graph first focused on the hydrograph pattern, which was followed by an inspection of the base flow and then of peak flow.

Following Haile et al. (2017), we also evaluated the model performance with the objective functions, Nash–Sutcliff model efficiency (NSE) and relative volumetric error (RVE). In this study, the model's ability to reproduce the pattern of the observed and predicted streamflow hydrographs was evaluated by using NSE. The volumetric error of the predicted streamflow was evaluated by using RVE.

The NSE values can range between 1.0 (perfect fit) and $-\infty$. An NSE value of less than zero indicates that the mean value of the observed time series would have been a better predictor than the model. The performance of the model is commonly considered very good (NSE > 0.8), good (0.6–0.8), satisfactory (0.5–0.6), and unsatisfactory (NSE < 0.5) (Pachepsky et al. 2016). NSE is defined as follows:

$$\mathrm{NSE} = 1 - \frac{\sum_{i=1}^{n} (Q_{\mathrm{O},i} - Q_{\mathrm{S},i})^2}{\sum_{i=1}^{n} (Q_{\mathrm{O},i} - \bar{Q}_{\mathrm{O},i})^2} \quad (3)$$

where $Q_{\mathrm{O},i}$ is the observed discharge at the time step i, $\bar{Q}_{\mathrm{O}}$ is the mean of the observed discharge, $Q_{\mathrm{S},i}$ is the simulation discharge at the time step i, and n is the number of observations.

RVE is estimated by

$$\mathrm{RVE} = \frac{\sum_{i=1}^{n} (Q_{\mathrm{S},i} - Q_{\mathrm{O},i})}{\sum_{i=1}^{n} Q_{\mathrm{O},i}} \times 100 \quad (4)$$

where all terms are as defined previously. The RVE values range between $-\infty$ and $+\infty$. The model performance is considered very good if the RVE value is between -5 and 5% and satisfactory when it is between 5 and 10% and -10 and -5%.

Standard periods are often defined for the impact study. These periods are historical (1971–2000), short-term (2011–2040), middle-term (2041–2070), and long-term (2071–2100). Since the short-term is already happening and the long-term is too far, our impact analysis focused more on the middle-term period. Climate change impact on streamflow was analyzed statistically at monthly, seasonally, and annual scales.

RESULTS

Model sensitivity to parameters

The HEC-HMS model sensitivity to its parameters was evaluated manually by changing the value of one model parameter at a time, while keeping the value of the remaining parameter constant. The sensitivity of those parameters was summarized in terms of the objective function, i.e. their effect on volume, pattern, and peak (Table 2). Simulated streamflow volume for the study area is most sensitive to the constant rate (CR) and moderately sensitive to the base flow (BF) parameter. Lag time, K, X, and initial

Table 2 | Summary of sensitive parameters of the model depending on objective criteria

Objective criteria	Parameters
Volume	Constant rate (CR) and Base flow (BF)
Pattern	Constant rate (CR), Base flow (BF), Lag time (Tlag), and Initial deficit (ID)
Peak flow	Constant rate (CR), Base flow (BF), and parameter X

deficit affect the simulated hydrograph pattern. The peak flow, volume, and pattern are affected by the constant rate (CR) and the base flow (BF).

Calibration and validation

The simulated and observed hydrographs for the calibration period are shown in Figure 3. Overall, the observed streamflow hydrograph is well simulated by the model. The rising and recession limbs of the simulated hydrograph are also well simulated, but the timing of the simulated hydrograph is not optimal. The main limitation of the model is in reproducing peak flows with noticeable underestimation for some years. We assume that the mismatch between the observed and the simulated hydrographs, particularly for high flows, will also be affected by the rating curve. We therefore suggest that the rating curve of the station must be revisited.

Model performance was found good in capturing the observed hydrograph pattern when evaluated by using NSE (NSE = 0.65). The RVE for the calibration period is 5.1%, which suggests that the model is highly efficient in estimating the observed streamflow volume. We consider that the percentage error in peak flow is 19%, which is relatively large. The model limitation and quality of observed data for peak flows may have contributed to the performance in simulating peaks.

Table 3 shows the optimized values of the HEC-HMS model of the study area. All parameter values are within the value ranges reported in the literature (e.g. Haile *et al.* 2017). The optimized values are not much less than the initial parameter values which were specified based on the literature and catchment characteristics.

The performance of the model in capturing the pattern of observed flow hydrograph during validation was satisfactory (NSE = 0.51). The model very well reproduced the observed flow volume (RVE = −6.1%) and percent error in peak flow (PEPF = 16%). The NSE and RVE values have slightly deteriorated during the validation compared with the calibration period (Table 4). It is common for objective function values to deteriorate during the validation period due to differences in model forcing conditions but where land use and land cover are unchanged. However, objective function values for the validation period indicate that the model can be used to evaluate the impact of climate change.

Evaluation of rainfall estimates from climate models

All four climate models failed to satisfactorily reproduce the observed annual rainfall of the Arjo-Didessa catchment (Figure 4). These models mostly underestimated the observed rainfall amount with notable underestimation for the rainy season. The peak monthly rainfall amount was captured only by HadGM2-ES. However, this model noticeably misses the start of the rainy season and ends earlier

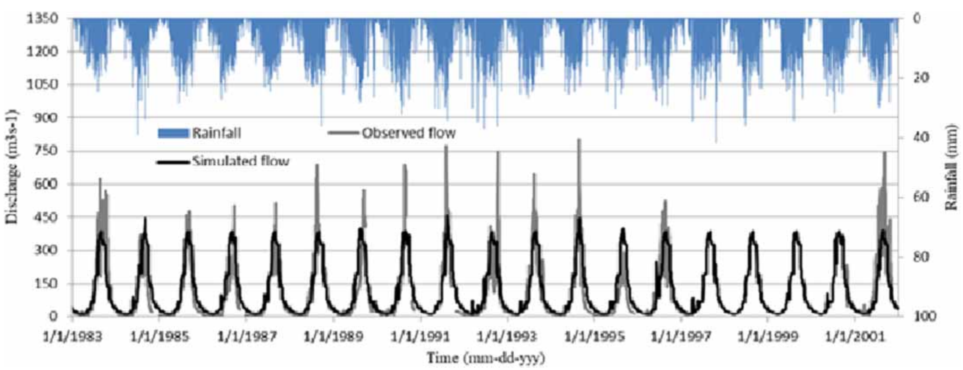

Figure 3 | Observed and simulated hydrographs for the calibration period (1983–2001).

Table 3 | Calibrated values of model parameters for the study area

Sub-basin	Reach	Parameters	Initial value	Optimized value
W40	–	Constant Rate (CR)	1.2	1.88
W50	–	Constant Rate (CR)	1.3	1.94
W80	–	Constant Rate (CR)	1.8	2.3
W90	–	Constant Rate (CR)	1.7	1.94
W40	–	Initial Deficit (ID)	3.2	3.27
W50	–	Initial Deficit (ID)	2.2	2.26
W80	–	Initial Deficit (ID)	4.2	4.26
W90	–	Initial Deficit (ID)	4.5	4.56
All	–	Maximum deficit (MD)	152	152.1
–	R20	K	140	140.23
–	R30	K	145	150
–	R20	X	0.15	0.085
–	R30	X	0.21	0.26
W40	–	Lag time (Tlag)	2,615	2,615
W50	–	Lag time (Tlag)	1,107	1,107
W80	–	Lag time (Tlag)	1,458	1,458.5
W90	–	Lag time (Tlag)	1,884.9	1,885

Note: The time lag is in min, the initial and maximum deficit is in mm, X (–), K is in h, and the constant rate is in cm/h. W40, W50, W80, and W90 are the sub-basins of Arjo-Didessa in Wama, Lower Arjo-Didessa, Middle Arjo-Didessa, and Upper Arjo-Didessa, respectively, while R20 and R30 are reached in the Middle and Lower Arjo-Didessa sub-basins.

Table 4 | Objective function values for the calibration and validation period

	Calibration		Validation	
Objective function	Value	Performance	Value	Performance
NSE (–)	0.66	Good	0.51	Satisfactory
R^2 (–)	0.85	Very good	0.85	Very good
RVE (%)	5.1	Very good	−6.1	Good
PEPF (%)	19	Good	16	Good

than reported by the observed data. Ensemble indicates the average daily rainfall of CM5A-MR, HadGM2-ES, ICHEC-EC, and CM5A-MR models output.

The annual rainfall of the Arjo-Didessa catchment is underestimated by as much as −34.8 to −72% with an average bias of −46.5% (Table 5). The largest bias was shown by the CM5A-MR model. The simulated annual rainfall is mostly more variable than the observed annual rainfall. HadGM2-ES showed the worst performance in reproducing

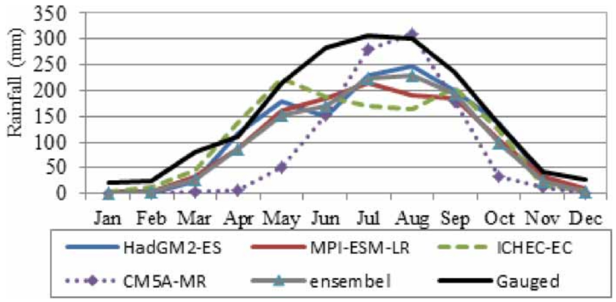

Figure 4 | Rainfall annual cycle over the Arjo-Didessa catchment from dynamically downscaled climate model simulations and gauged data on a monthly basis.

Table 5 | Accuracy of the climate models in reproducing mean annual rainfall over the Arjo-Didessa catchment over the period (1981–2005)

	Annual rainfall (mm)	Bias (%)	CV (%)	RMSE (mm year^{-1})	Correlation (–)
Gauged	1,779	–	7.6	–	–
HadGM2-ES	1,320	−34.8	17.2	373	−0.312
MPI-ESM-LR	1,209	−47.2	10.7	431	−0.080
ICHEC-EC	1,296	−37.3	6.0	334	0.354
CM5A-MR	1,037	−71.6	13.2	599	−0.316
Ensemble	1,215	−46.4	6.5	412	−0.306

the temporal variability (CV = 17.2%) of the annual rainfall amount (CV = 7.6%). The performance of the models was also unsatisfactory when evaluated by RMSE and CC. These values indicate that the simulated rainfall over the catchment is not fit for direct use for our climate change impact study, but that bias correction is needed.

Climate change impact

The climate models do not agree in terms of both the magnitude and direction of the future change in annual rainfall amount for the medium-future period 2041–2070 (Figure 5). These inter-model differences in predicting future changes are likely to be a result of using different climate model approaches and subsequent parameterizations (Haile *et al.* 2017). CM5A-MR and ICHEC-EC projections show a slight or small change in rainfall amount (−16 to +1.7%) under the RCP 4.5 climate projection scenario. However, there will be a significant decline (up to 21%) in annual rainfall of the study area according to MPI-ESM-

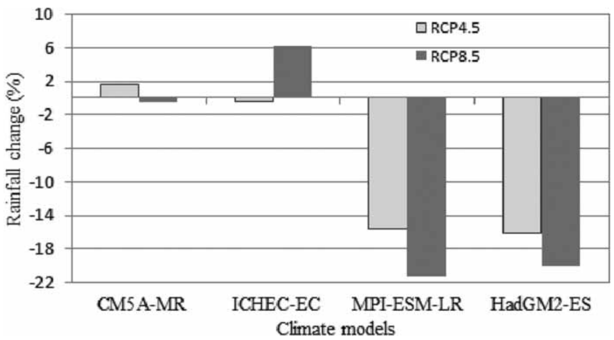

Figure 5 | Projected changes in the annual catchment rainfall of the Arjo-Didessa catchment over the period 2041–2070.

LR and HadGM2-ES models under RCP 8.5. Almost a similar result is reported by Tariku *et al.* (2021), i.e. −10.3 to 19.4%.

All climate model projections indicate that the minimum and maximum temperatures of the Arjo-Didessa catchment are likely to increase for the period 2041–2070. This is consistent in both climate scenarios. The projected increment of maximum temperature is between 1.2 and 1.3 °C under RCP 4.5 and 1.5 and 3.2 °C under RCP 8.5. The minimum temperature will increase by 0.98 to 1.2 °C under the RCP 4.5 scenario, whereas it will increase by 1.2 to 1.5 °C under the RCP 8.5 scenario. The change in temperature over the UBN is exactly similar in direction for many studies and nearly similar in magnitude with an increase of 4.1 °C. For example, Chakilu *et al.* (2020), Worqlul *et al.* (2018), and Roth *et al.* (2018) reported that the change in temperature is between 0.84 and 4.1 °C.

The increase in temperature will be followed by a likely increase in annual evapotranspiration of the study area (Figure 6). The increment is 3 to 5% under the RCP 4.5 scenario, while it slightly increases under RCP 8.5. CM5A-MR projected the largest increase in PET, while ICHEC-EC reported the smallest increment.

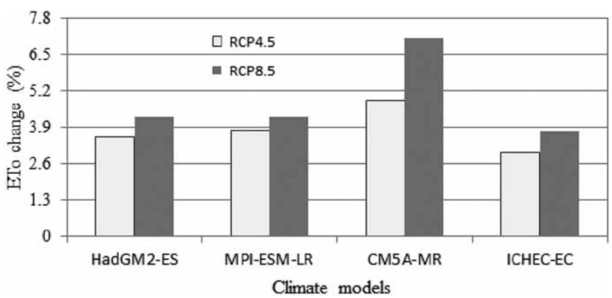

Figure 6 | Annual average evapotranspiration change of the Arjo-Didessa catchment over the period 2041–2070.

Under RCP 4.5, the reported direction of annual streamflow changes shows agreement for all models, except for CM5A-MR (Figure 7). The three models' projection suggests that the annual streamflow is likely to decrease by small amounts (1 to 3%) in 2041–2070. Similarly, the streamflow of Bega (dry) and Belg (small rain) seasons will slightly decrease (mostly by less than 2%). However, there is a projected increase of flow in Kiremt (the main rainy season) by 3.5 to 5%. Seasonal flow increases in magnitude in the rainy season is called 'Kiremt'.

Under RCP 8.5, the reported direction of annual streamflow changes shows agreement for all models, except for ICHEC-EC (Figure 8). All models projected a slight decline of flow in the Bega season, while the result is mixed for Belg. However, the results of all models show that streamflow will increase in Kiremet even though there is a significant difference in the magnitude of change between the models. In Kiremt, runoff over the catchment is projected to increase by up to 18%.

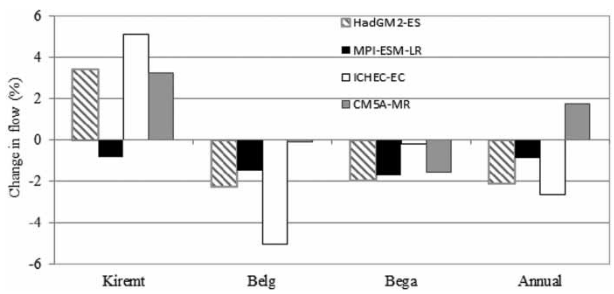

Figure 7 | Change in seasonal and annual streamflow for the medium future (2041–2070) under the RCP 4.5 scenario.

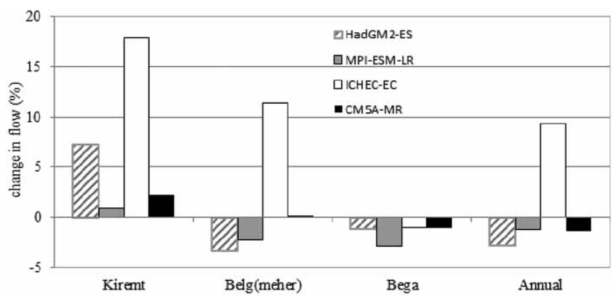

Figure 8 | Change in seasonal and annual streamflow for the medium future (2041–2070) under the RCP 8.5 scenario.

CONCLUSION

In this study, we evaluated the impact of climate change on the streamflow of the Arjo-Didessa catchment for the medium-future period 2041–2070 under the RCP 4.5 and RCP 8.5 scenarios. The HEC-HMS model was used to simulate historical and future runoff using the downscaled dynamically climate data obtained from the HadGM2-ES, MPI-ESM-LR, CM5A-MR, and ICHEC-EC GCM models. Downscaled data were from CCLM, RCA4, and RACMO22 T RCMs and were available through CORDEX (http://wcrp-cordex.ipsl.jussieufr).

The calibrated HEC-HMS model well captured the observed hydrograph pattern (NSE = 0.65) and the observed hydrograph volume (RVE = 5.1%). The model performance for the validation period was acceptable. Hence, the HEC-HMS model was used to evaluate the climate change impact on the streamflow of the Arjo-Didessa catchment.

The climate models did not satisfactorily capture the monthly rainfall pattern, volume, and peak of the study area. The annual rainfall amount was significantly underestimated, while there was also a weak linear relationship between the simulated and the observed annual rainfall amount (correlation = −0.08 to −0.354). We, therefore, applied bias correction to the rainfall and temperature data of the climate models before further analysis.

The four climate models show agreement in the magnitude and direction of projected change for the medium future (2041–2070) in the annual rainfall amount of the study area under RCP 4.5. The annual rainfall is projected to increase by 0.36 to 2%. Similar results (−2.8 to +2.7%) were reported by Haile *et al.* (2017) from six climate models under the RCP 4.5 scenario in the medium future (2041–2070) over the UBN basin. Teklesadik *et al.* (2017) reported from the analysis of global climate models that the annual rainfall of the UBN basin will increase by 4 to 10% for the future period. Similarly, Gebre *et al.* (2015) concluded that the average annual rainfall of the Didessa catchment may increase by 8.4% using outputs from the single GCM (ECHAM5) under the A1B scenario. The projected changes in annual rainfall were not conclusive under RCP 8.5.

The daily maximum temperature is projected to increase by 1.17 to 1.39 °C under the RCP 4.5 scenario. The minimum temperature is projected to increase by 0.98 to 1.24 °C. Consequently, the annual PET will increase by 3 to 5%. The magnitude of PET change in this study is much smaller than that in some previous studies (Nawaz *et al.* 2010, +30%; Haile *et al.* 2017, +8.6%), while Teklesadik *et al.* (2017) and Worqlul *et al.* (2018) reported that PET will increase by 4.4 and 7.8%, respectively, which is almost similar to the results reported in this study. We noticed that these previous investigations were done over the meso-scale UBN basin. Temperature and PET will also increase under RCP 8.5 but with a larger magnitude of change than under RCP 4.5.

Changes in monthly streamflow are more pronounced (up to 27%) than annual changes. The projected changes also vary with season. Our findings on the monthly change of streamflow are significantly smaller than those reported by Eregno *et al.* (2013) (−50 to +30%) and Mengistu *et al.* (2020) (up to −27%).

Under RCP 4.5, the annual streamflow of the study area is projected to decrease by small amounts (<3%). There will also be a decrease in the flows of the dry season and the small rainy season. However, the future flow will be higher than historic flows (by up to 5%) in the main rainy season. The results are also similar to those for RCP 8.5 despite some inconsistencies between the projections of the climate models. The annual streamflow magnitude that we report in this study is different in both direction and magnitude to a result reported by Gebre *et al.* (2015) (+13.7%) and the same in direction but smaller in magnitude to that reported by Adgolign *et al.* (2016) (−10%), while it is almost similar in magnitude but different in direction to the result reported by Chakilu *et al.* (2020) (4.06, 3.26, and 3.67% under the RCP 2.6, RCP 4.5, and RCP 8.5 scenarios, respectively). These differences mainly result from the use of different climate scenarios and GCMs.

The magnitude of climate change impact in the Arjo-Didessa catchment under the RCP scenarios, as reported here, is smaller than that reported for the UBN basin under the SRES scenario (e.g. Abdo *et al.* 2009; Elshamy *et al.* 2009; Worqlul *et al.* 2018). However, the projected changes in streamflow cannot be ignored in future water resources management of the study area. Particularly, the monthly and seasonal changes of streamflow are still considerable under RCP scenarios.

AUTHOR CONTRIBUTIONS

Conceptualization: Alemseged Tamiru Haile and Wudeneh Temesgen Bekele; Formal Analysis: Wudeneh Temesgen Bekele; Paper Preparation: Wudeneh Temesgen Bekele, Alemseged Tamiru Haile, and Tom Rientjes.

CONFLICTS OF INTEREST

The authors declare no conflict of interest.

FUNDING

This research received no external funding.

DATA AVAILABILITY STATEMENT

All relevant data are included in the paper or in its Supplementary Information.

REFERENCES

Abdo, K., Fiseha, B., Rientjes, T., Gieske, A. & Haile, A. 2009 Assessment of climate change impacts on the hydrology of Gilgel Abay catchment in Lake Tana basin, Ethiopia. *Hydrological Processes* **23**, 3661–3669.

Adgolign, T. B., Rao, G. S. & Abbulu, Y. 2016 WEAP modeling of surface water resources allocation in Didessa Sub-Basin, West Ethiopia. *Sustainable Water Resources Management* **2** (1), 55–70.

Aich, V., Liersch, S., Vetter, T., Huang, S., Tecklenburg, J., Hoffmann, P., Koch, H., Fournet, S., Krysanova, V. & Müller, E. 2014 Comparing impacts of climate change on streamflow in four large African river basins. *Hydrology and Earth System Sciences* **18**, 1305.

Beyene, T., Lettenmaier, D. P. & Kabat, P. 2010 Hydrologic impacts of climate change on the Nile River Basin: implications of the 2007 IPCC scenarios. *Climatic Change* **100**, 433–461.

Chakilu, G. G., Sándor, S. & Zoltán, T. 2020 Nov Change in streamflow of Gumara watershed, upper Blue Nile Basin, Ethiopia under representative concentration pathway climate change scenarios. *Water* **12** (11), 3046.

Change, I. C. 2014 IPCC. Impacts, Adaptation and Vulnerability, IPCC WGII AR5 Summary for Policymakers. IPCC.

Chow, V. T., Maidment, D. R. & Mays, L. W. 1988 *Applied Hydrology*. McGraw-Hill, New York, NY.

Elshamy, M. E., Seierstad, I. A. & Sorteberg, A. 2009 Impacts of climate change on Blue Nile flows using bias-corrected GCM scenarios. *Hydrology and Earth System Sciences* **13** (5), 551–565. doi:10.5194/hess-13-551-2009.

Enyew, B., Van lanen, H. & Van loon, A. 2014 Assessment of the impact of climate change on hydrological drought in Lake Tana catchment, Blue Nile basin, Ethiopia. *Journal of Geology and Geoscience* **3**, 174.

Eregno, F. E., Xu, C. Y. & Kitterød, N.O. 2020 Modeling hydrological impacts of climate change in different climatic zones. *International Journal of Climate Change Strategies and Management* **5** (3), 344–365.

Gebre, S., Tadele, K. & Mariam, B. 2015 Potential impacts of climate change on the hydrology and water resources availability of Didessa catchment, Blue Nile River Basin, Ethiopia. *Journal of Geology and Geoscience* **4**, 193.

Gelete, G., Gokcekus, H. & Gichamo, T. 2020 Impact of climate change on the hydrology of Blue Nile basin, Ethiopia: a review. *Journal of Water and Climate Change* **11** (4), 1539–1550.

Haile, A. T., Akawka, A. L., Berhanu, B. & Rientjes, T. 2017 Changes in water availability in the Upper Blue Nile basin under the representative concentration pathways scenario. *Hydrological Sciences Journal* **62** (13), 2139–2149.

Kim, U. & Kaluarachchi, J. J. 2009 Climate change impacts on water resources in the Upper Blue Nile River Basin, Ethiopia. *JAWRA* **45**, 1361–1378.

Lafon, T., Dadson, S., Buys, G. & Prudhomme, C. 2013 Bias correction of daily precipitation simulated by a regional climate model: a comparison of methods. *International Journal of Climatology* **33**, 1367–1381.

McCartney, M. P. & Menker Girma, M. 2012 Evaluating the downstream implications of planned water resource development in the Ethiopian portion of the Blue Nile River. *Water International* **37**, 362–379.

Mengistu, D., Bewket, W., Dosio, A. & Panitz, H. J. 2020 Climate change impacts on water resources in the Upper Blue Nile (Abay) River Basin, Ethiopia. *Journal of Hydrology* **592**, 125614.

Nawaz, N., Bellerby, T., Sayed, M. & Elshamy, M. 2010 Blue Nile runoff sensitivity to climate change. *The Open Hydrology Journal* **4**, 137–151.

Pachepsky, Y. A., Martinez, G., Pan, F., Wagener, T. & Nicholson, T. 2016 Evaluating hydrological model performance using information theory-based metrics. *Hydrology and Earth System Sciences*. Discussion. [preprint]. https://doi.org/10.5194/hess-2016-46.

Razmkhah, H., Akhoond, A. A., Saghafian, B. & Radmanesh, F. 2014 Comparing the performance of different loss models in the rainfall-runoff modeling of the Karoon III Basin. *Water Resources Engineering* **12**, 17–35.

Rogelj, J., Meinshausen, M. & Knutti, R. 2012 Global warming under old and new scenarios using IPCC climate sensitivity range estimates. *Nature Climate Change* **2**, 248–253. doi:10.1038/nclimate1385.

Roth, V., Lemann, T., Zeleke, G., Subhatu, A. T., Nigussie, T. K. & Hurni, H. 2018 Effects of climate change on water resources in the upper Blue Nile Basin of Ethiopia. *Heliyon* **4** (9), e00771.

Rui, X. & Wang, L. 2000 A study of flood routing method with forecast period. *Advances in Water Science* **11**, 291–295.

Saleh, A., Ghobad, R. & Noredin, R. 2011 Evaluation of HEC-HMS methods in surface runoff simulation (Case study: Kan watershed, Iran). *Advances in Environmental Biology* **5**, 1316–1322.

Setegn, S. G., Rayner, D., Melesse, A. M., Dargahi, B. & Srinivasan, R. 2011 Impact of climate change on the hydroclimatology of Lake Tana Basin, Ethiopia. *Water Resources Research* **47**.

Shaka, A. K. 2008 Assessment of climate change impacts on the hydrology of gilgel Abbay catchment in Lake Tana basin, Ethiopia. ITC. PhD Thesis. https://webapps.itc.utwente.nl/librarywww/papers_2008/msc/wrem/abdo.pdf.

Tariku, T. B., Gan, T. Y., Li, J. & Qin, X. 2021 Impact of climate change on Hydrology and Hydrologic Extremes of Upper Blue Nile River Basin. *Journal of Water Resources Planning and Management* **147** (2), 04020104.

Taye, M. T., Willems, P. & Block, P. 2015 Implications of climate change on hydrological extremes in the Blue Nile basin: a review. *Journal of Hydrology: Regional Studies* **4**, 280–293.

Teklesadik, A. D., Alemayehu, T., Van Griensven, A., Kumar, R., Liersch, S., Eisner, S., Tecklenburg, J., Ewunte, S. & Wang, X. 2017 Inter-model comparison of hydrological impacts of climate change on the Upper Blue Nile basin using ensemble of hydrological models and global climate models. *Climatic Change* **141** (3), 517–532.

Terink, W., Hurkmans, R., Torfs, P. & Uijlenhoet, R. 2010 Evaluation of a bias correction method applied to downscaled precipitation and temperature reanalysis data for the Rhine basin. *Hydrology and Earth System Sciences* **14**, 687–703.

Teutschbein, C. & Seibert, J. 2012 Bias correction of regional climate model simulations for hydrological climate-change impact studies: review and evaluation of different methods. *Journal of Hydrology* **456**, 12–29.

Thomson, A. M., Calvin, K. V., Smith, S. J., Kyle, G. P., Volke, A., Patel, P., Delgado-Arias, S., Bond-Lamberty, B., Wise, M. A. & Clarke, L. E. 2011 RCP4.5: a pathway for stabilization of radiative forcing by 2100. *Climatic Change* **109**, 77.

Tisseuil, C., Vrac, M., Lek, S. & Wade, A. J. 2010 Statistical downscaling of river flows. *Journal of Hydrology* **385**, 279–272.

Worqlul, A. W., Dile, Y. T., Ayana, E. K., Jeong, J., Adem, A. A. & Gerik, T. 2018 Impact of climate change on streamflow hydrology in headwater catchments of the Upper Blue Nile Basin, Ethiopia. *Water* **10**, 120.

First received 28 October 2020; accepted in revised form 23 February 2021. Available online 15 March 2021